

# Determination of matter radius and neutron-skin thickness of $^{60,62,64}\text{Ni}$ from reaction cross section of proton scattering on $^{60,62,64}\text{Ni}$ targets

Shingo Tagami

Department of Physics, Kyushu University, Fukuoka 819-0395, Japan

Tomotsugu Wakasa

Department of Physics, Kyushu University, Fukuoka 819-0395, Japan

Masanobu Yahiro\*

Department of Physics, Kyushu University, Fukuoka 819-0395, Japan

(Dated: July 12, 2023)

**Background:** In our previous work, we determined matter radii  $r_m(\text{exp})$  and neutron-skin thickness  $r_{\text{skin}}(\text{exp})$  from reaction cross sections  $\sigma_R(\text{exp})$  of proton scattering on  $^{208}\text{Pb}$ ,  $^{58}\text{Ni}$ ,  $^{40,48}\text{Ca}$ ,  $^{12}\text{C}$  targets, using the chiral (Kyushu)  $g$ -matrix folding model with the densities calculated with Gogny-D1S-HFB (D1S-GHFB) with angular momentum projection (AMP). The resultant  $r_{\text{skin}}(\text{exp})$  agree with the PREX2 and CREX values. As for  $^{58}\text{Ni}$ , our value is consistent with one determined from the differential cross section for  $^{58}\text{Ni}+^4\text{He}$  scattering. As for  $p+^{60,62,64}\text{N}$  scattering,  $\sigma_R(\text{exp})$  are available as a function of incident energies  $E_{\text{in}}$ , where  $E_{\text{in}} = 22.8 \sim 65.5$  MeV for  $^{60}\text{Ni}$ ,  $E_{\text{in}} = 40, 60.8$  MeV for  $^{62}\text{Ni}$ ,  $E_{\text{in}} = 40, 60.8$  MeV for  $^{64}\text{Ni}$ .

**Purpose:** Our aim is to determine matter radii  $r_m(\text{exp})$  for  $^{60,62,64}\text{Ni}$  from the  $\sigma_R(\text{exp})$ .

**Method:** Our method is the Kyushu  $g$ -matrix folding model with the densities scaled from D1S-GHFB+AMP densities,

**Results:** Our skin values are  $r_{\text{skin}}(\text{exp}) = 0.076 \pm 0.019, 0.106 \pm 0.192, 0.162 \pm 0.176$  fm, and  $r_m(\text{exp}) = 3.759 \pm 0.011, 3.811 \pm 0.107, 3.864 \pm 0.101$  fm for  $^{60,62,64}\text{Ni}$ , respectively.

## I. INTRODUCTION AND CONCLUSION

### A. Background

*Background:* A novel method for measuring nuclear reactions in inverse kinematics with stored ion beams was successfully used to extract the matter radius  $r_m(\text{exp})$  of  $^{58}\text{Ni}$  [1]. The experiment was performed at the experimental heavy-ion storage ring at the GSI facility. Their result determined from the differential cross section for  $^{58}\text{Ni}+^4\text{He}$  scattering is  $r_m(\text{GSI}) = 3.70(7)$  fm.

Reaction cross section  $\sigma_R$  is a standard observable to determine  $r_m(\text{exp})$  and neutron-skin thickness  $r_{\text{skin}}(\text{exp})$ ; note that  $r_{\text{skin}}$  can be evaluated from the  $r_m$  by using the  $r_p(\text{exp})$  calculated with the isotope shift method based on the electron scattering [2]. In fact, we determined  $r_m(\text{exp})$  and  $r_{\text{skin}}(\text{exp})$  from  $\sigma_R(\text{exp})$  of proton scattering on  $^{208}\text{Pb}$ ,  $^{58}\text{Ni}$ ,  $^{40,48}\text{Ca}$ ,  $^{12}\text{C}$  targets, using the chiral (Kyushu)  $g$ -matrix folding model with the proton and neutron densities scaled with D1S-GHFB+AMP densities [3], where D1S-GHFB+AMP is the abbreviation of Gogny-D1S-HFB with angular momentum projection (AMP). Our skin values  $r_{\text{skin}}(\text{exp})$  agree with the PREX2 and CREX values. As for  $^{58}\text{Ni}$ , our matter radius  $r_m(\text{exp}) = 3.711 \pm 0.010$  fm. is consistent with  $r_m(\text{GSI}) = 3.70(7)$  fm. As for  $p+^{60,62,64}\text{N}$  scattering,  $\sigma_R(\text{exp})$  are available as a function of incident energy  $E_{\text{in}}$ [4–6]; here  $E_{\text{in}} = 22.8 \sim 65.5$  MeV for  $^{60}\text{Ni}$ ,  $E_{\text{in}} = 40, 60.8$  MeV for  $^{62}\text{Ni}$ ,  $E_{\text{in}} = 40, 60.8$  MeV for  $^{64}\text{Ni}$ . Now we consider  $p+^{60,62,64}\text{N}$  scattering.

*Purpose:* Our aim is to determine  $r_m(\text{exp})$ ,  $r_{\text{skin}}(\text{exp})$  for  $^{60,62,64}\text{Ni}$  from the  $\sigma_R(\text{exp})$  by using the Kyushu  $g$ -matrix folding model with the proton and neutron densities scaled from D1S-GHFB+AMP ones.

*Results:* Our results  $r_m(\text{exp})$ ,  $r_n(\text{exp})$ ,  $r_{\text{skin}}(\text{exp})$  are listed in Table I.

*Conclusion* We discover the fact the  $r_m(\text{exp})/A^{1/3}$  (the matter radius per nucleon) is inversely proportional to the total binding energy per nucleon  $E_B/A$ , where  $A$  is the mass number.

TABLE I. Values of  $r_m$ ,  $r_n$ ,  $r_{\text{skin}}$ ,  $r_p$ . The  $r_p(\text{exp})$  are determined from the charge radii [2]. ‘Data’ shows citations on  $\sigma_R$ . The radii are shown in units of fm.

	$r_p(\text{exp})$	$r_m(\text{exp})$	$r_n(\text{exp})$	$r_{\text{skin}}(\text{exp})$	Data
$^{58}\text{Ni}$	3.6849	$3.711 \pm 0.010$	$3.740 \pm 0.019$	$0.055 \pm 0.019$	[3]
$^{60}\text{Ni}$	3.723	$3.759 \pm 0.011$	$3.799 \pm 0.019$	$0.076 \pm 0.019$	[4, 5]
$^{62}\text{Ni}$	3.753	$3.811 \pm 0.107$	$3.859 \pm 0.192$	$0.106 \pm 0.192$	[6]
$^{64}\text{Ni}$	3.772	$3.864 \pm 0.101$	$3.933 \pm 0.176$	$0.162 \pm 0.176$	[6]

## II. FOLDING MODEL

Kohno calculated the  $g$  matrix for the symmetric nuclear matter, using the Brueckner-Hartree-Fock method with chiral  $\text{N}^3\text{LO}$  2NFs and NNLO 3NFs [7]. He set  $c_D = -2.5$  and  $c_E = 0.25$  so that the energy per nucleon can become minimum at  $\rho = \rho_0$ . Toyokawa *et al.* localized the non-local chiral  $g$  matrix [8], using the localization procedure proposed

\* orion093g@gmail.com

by the Melbourne group [9, 10]. The resulting local  $g$  matrix is referred to as “local Kyushu  $g$ -matrix”.

We use the Kyushu  $g$ -matrix folding model [8] with the densities calculated with D1S-GHFB+AMP [11]. The Kyushu  $g$ -matrix itself [8] is constructed from the chiral nucleon-nucleon (NN) interaction with the cutoff 550 MeV.

In this paper, we consider proton-nucleus scattering. The potential  $U(\mathbf{R})$  consists of the direct and exchange parts,  $U^{\text{DR}}(\mathbf{R})$  and  $U^{\text{EX}}(\mathbf{R})$  [12, 13]. The validity of the localization is shown in Refs. [12].

### A. Scaling procedure of proton and neutron densities

For example, the neutron density  $\rho_n(r)$  is scaled from the D1S-GHFB+AMP one. We can obtain the scaled density  $\rho_{\text{scaling}}(\mathbf{r})$  from the original density  $\rho(\mathbf{r})$  as

$$\rho_{\text{scaling}}(\mathbf{r}) = \frac{1}{\alpha^3} \rho(\mathbf{r}/\alpha) \quad (1)$$

with a scaling factor

$$\alpha = \sqrt{\frac{\langle r^2 \rangle_{\text{scaling}}}{\langle r^2 \rangle}}. \quad (2)$$

We scale the neutron density so that the  $f \times \sigma_{\text{R}}(\text{D1S})$  may reproduce the data ( $\sigma_{\text{R}}(\text{exp})$ ) under that condition that the  $r_{\text{p}}(\text{scaling})$  agrees with  $r_{\text{p}}(\text{exp})$  [2] of electron scattering, where  $\sigma_{\text{R}}(\text{D1S})$  is the result of D1S-GHFB+AMP for each  $E_{\text{in}}$ . and  $f$  is the average of  $\sigma_{\text{R}}(\text{exp})/\sigma_{\text{R}}(\text{D1S})$  over  $E_{\text{in}}$ . The matter radius  $r_{\text{m}}(E_{\text{in}})$  thus obtained depends on  $E_{\text{in}}$ . We then take the average of  $r_{\text{m}}(E_{\text{in}})$  over  $E_{\text{in}}$ . The resulting value  $r_{\text{m}}(\text{exp})$  is shown in Table I. The corresponding  $r_{\text{n}}(\text{exp})$  and  $r_{\text{skin}}(\text{exp})$  obtained from  $r_{\text{m}}(\text{exp})$  and  $r_{\text{p}}(\text{exp})$  are also shown in Table I.

D1M [14, 15] is an improved version of D1S for binding energies of many nuclei. We can use D1M instead of D1S, leading to the change of  $U(\mathbf{R})$ . The results of D1M are the same as our results of Table I.

This scaling procedure is used for proton scattering on Sn in Ref. [16].

## III. RESULTS

Figure 1 shows reaction cross sections  $\sigma_{\text{R}}$  as a function of  $E_{\text{in}}$ . Our result  $\sigma_{\text{R}}(\text{D1S})$  overshoots somewhat, but  $f \times \sigma_{\text{R}}(\text{D1S})$  is close to the central values of experimental data [4, 5], where  $f = 0.97488$ . The  $f \times \sigma_{\text{R}}(\text{D1S})$  are used in order to determine  $r_{\text{m}}(\text{exp})$  and  $r_{\text{skin}}(\text{exp})$ .

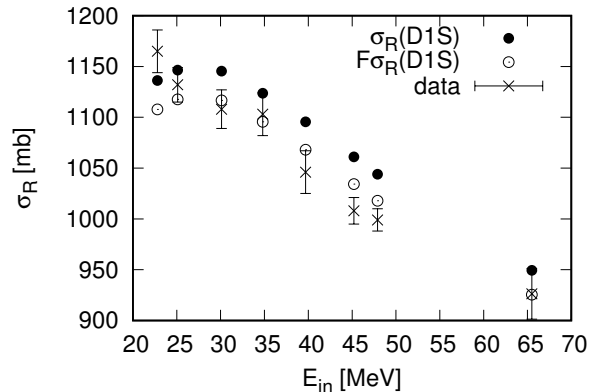


FIG. 1.  $E_{\text{in}}$  dependence of reaction cross sections  $\sigma_{\text{R}}$  for  $p+^{60}\text{Ni}$  scattering. Closed circles denote  $\sigma_{\text{R}}(\text{D1S})$  of the D1S-GHFB+AMP densities, whereas open circles correspond to  $f \times \sigma_{\text{R}}(\text{D1S})$ . The data (crosses) are taken from Refs. [4, 5].

The same scaling procedure is taken also for  $p+^{62,64}\text{Ni}$  scattering, where  $F = 0.96213, 0.98232$  for  $^{62,64}\text{Ni}$ , respectively.

The data on  $E_{\text{B}}/A$  (the total binding energy per nucleon) weakly depend on  $A$  for  $^{58,60,62,64}\text{Ni}$  [17]. This is true for  $r_{\text{m}}(\text{exp})/A^{1/3}$  (the matter radius per nucleon). In fact,  $A$  dependence of  $r_{\text{m}}(\text{exp})/A^{1/3} \times E_{\text{B}}/A$  is even smaller; namely, the average  $\beta$  of  $r_{\text{m}}(\text{exp})/A^{1/3} \times E_{\text{B}}/A$  over  $A$  is

$$\beta = 8.437385 \text{ MeV} \cdot \text{fm} \quad (3)$$

and the error is  $0.024 \text{ MeV} \cdot \text{fm}$ . The relative error is  $0.2847\%$ . This indicates that the  $r_{\text{m}}(\text{exp})/A^{1/3}$  (the matter radius per nucleon) is in inverse proportional to the total binding energy per nucleon  $E_{\text{B}}/A$ ; see Table II for  $E_{\text{B}}/A$  and  $r_{\text{m}}(\text{exp})/A^{1/3}$ .

Using  $\beta = 8.437385 \text{ MeV} \cdot \text{fm}$ ,  $E_{\text{B}}/A$ , we can derive the central values of  $r_{\text{m}}(\text{exp})$ . These are  $3.711, 3.759, 3.811, 3.864 \text{ fm}$  for  $^{58,60,62,64}\text{Ni}$ . These values agree with our values of Table I. One can easily evaluate the central value of matter radius from  $\beta$ ,  $E_{\text{B}}/A$ . This is convenient.

TABLE II. Values of  $E_{\text{B}}/A$  [17],  $r_{\text{m}}(\text{exp})/A^{1/3}$ . The  $r_{\text{m}}(\text{exp})$  are shown in units of fm and the  $E_{\text{B}}/A$  are in MeV.

	$BE/A$	$r_{\text{m}}(\text{exp})/A^{1/3}$
$^{58}\text{Ni}$	8.732059	0.959
$^{60}\text{Ni}$	8.780774	0.960
$^{62}\text{Ni}$	8.794553	0.963
$^{64}\text{Ni}$	8.777461	0.966

## ACKNOWLEDGMENTS

We would like to thank Dr. Toyokawa for his contribution.

- 
- [1] J. C. Zamora *et al.*, Nuclear-matter radius studies from Ni58( $\alpha,\alpha$ ) experiments at the GSI Experimental Storage Ring with the EXL facility, *Phys. Rev. C* **96**, 034617 (2017).
- [2] I. Angeli and K. P. Marinova, Table of experimental nuclear ground state charge radii: An update, *Atom. Data Nucl. Data Tabl.* **99**, 69 (2013).
- [3] T. Wakasa, S. Tagami, J. Matsui, M. Takechi, and M. Yahiro, Neutron-skin values and matter and neutron radii determined from reaction cross sections of proton scattering on  $^{12}\text{C}$ ,  $^{40,48}\text{Ca}$ ,  $^{58}\text{Ni}$ , and  $^{208}\text{Pb}$ , *Phys. Rev. C* **107**, 024608 (2023).
- [4] A. Ingemarsson, J. Nyberg, P. Renberg, O. Sundberg, R. Carlson, A. Auce, R. Johansson, G. Tibell, B. Clark, L. Kurth Kerr, and S. Hama, *Nuclear Physics A* **653**, 341 (1999).
- [5] T. Eliyakut-Roshko, R. H. McCamis, W. T. H. van Oers, R. F. Carlson, and A. J. Cox, Measurements of proton total reaction cross sections for  $^{58}\text{Ni}$  and  $^{60}\text{Ni}$  including nonrelativistic and relativistic data analyses, *Phys. Rev. C* **51**, 1295 (1995).
- [6] J. J. H. Menet, E. E. Gross, J. J. Malanify, and A. Zucker, Total-reaction-cross-section measurements for 30-60-mev protons and the imaginary optical potential, *Phys. Rev. C* **4**, 1114 (1971).
- [7] M. Kohno, Strength of reduced two-body spin-orbit interaction from chiral three-nucleon force, *Phys. Rev. C* **86**, 061301 (2012), arXiv:1209.5048 [nucl-th].
- [8] M. Toyokawa, M. Yahiro, T. Matsumoto, and M. Kohno, Effects of chiral three-nucleon forces on  $^4\text{He}$ -nucleus scattering in a wide range of incident energies, *PTEP* **2018**, 023D03 (2018), arXiv:1712.07033 [nucl-th].
- [9] H. V. von Geramb *et al.*, *Phys. Rev. C* **44**, 73 (1991).
- [10] K. Amos and P. J. Dortmans, *Phys. Rev. C* **49**, 1309 (1994).
- [11] S. Tagami, M. Tanaka, M. Takechi, M. Fukuda, and M. Yahiro, Chiral  $g$ -matrix folding-model approach to reaction cross sections for scattering of Ca isotopes on a C target, *Phys. Rev. C* **101**, 014620 (2020), arXiv:1911.05417 [nucl-th].
- [12] K. Minomo, K. Ogata, M. Kohno, Y. R. Shimizu, and M. Yahiro, The Brieva-Rook Localization of the Microscopic Nucleon-Nucleus Potential, *J. Phys. G* **37**, 085011 (2010), arXiv:0911.1184 [nucl-th].
- [13] S. Watanabe *et al.*, Ground-state properties of neutron-rich Mg isotopes, *Phys. Rev. C* **89**, 044610 (2014), arXiv:1404.2373 [nucl-th].
- [14] S. Goriely, S. Hilaire, M. Girod, and S. Peru, First Gogny-Hartree-Fock-Bogoliubov Nuclear Mass Model, *Phys. Rev. Lett.* **102**, 242501 (2009).
- [15] L. M. Robledo, T. R. Rodríguez, and R. R. Rodríguez-Guzmán, Mean field and beyond description of nuclear structure with the Gogny force: A review, *J. Phys. G* **46**, 013001 (2019), arXiv:1807.02518 [nucl-th].
- [16] S. Tagami, T. Wakasa, and M. Yahiro, Neutron skin thickness of 116,118,120,122,124sn determined from reaction cross sections of proton scattering, *Results in Physics* **46**, 106296 (2023).
- [17] <https://www.nndc.bnl.gov/nudat2/>.